



An Insight into Photophysical Investigation of (*E*)-2-Fluoro-*N'*-(1-(4-Nitrophenyl)Ethylidene)Benzohydrazide through Solvatochromism Approaches and Computational Studies

Ditto Abraham Thadathil¹ · Shanu Varghese¹ · K B Akshaya¹ · Renjith Thomas² · Anitha Varghese¹ 

Received: 6 March 2019 / Accepted: 8 July 2019 / Published online: 15 July 2019
© Springer Science+Business Media, LLC, part of Springer Nature 2019

Abstract

A fluoro-based Schiff base (*E*)-2-fluoro-*N'*-(1-(4-nitrophenyl)ethylidene)benzohydrazide (FNEB) has been synthesized from condensation of 2-fluorobenzohydrazide and 4'-nitroacetophenone catalyzed by glacial acetic acid with ethanol as the solvent. The dipole moment of FNEB in both the electronic states were found using different solvatochromic approaches such as Lippert-Mataga, Bakhshiev, Kawski-Chamma-Viallet, Reichardt and Bilot-Kawski. The experimental ground state dipole moment of FNEB was calculated using Guggenheim-Debye method and theoretical ground state dipole moment using Bilot-Kawski solvatochromic approach. The solvatochromic behavior of the Schiff base in different solvents was studied using absorption and emission spectra. Catalan and Kamlet-Abboud-Taft parameters were used from the multiple linear regression (MLR) analysis in order to study the solute-solvent interaction. The dipole moments were also calculated using Time Dependent-Density Functional Theory (TD-DFT). The chemical stability of FNEB was determined using computational and Cyclic Voltammetry by the use of obtained energy gap between the frontier orbitals. Using the frontier orbitals energy gap, global reactivity parameters were computed. Further, Light Harvesting efficiency was determined to comprehend the photovoltaic property of the Schiff base.

Keywords Schiff base · Guggenheim-Debye method · Solvatochromic method · Photophysical properties · TD-DFT · Light harvesting efficiency

Introduction

The scientific concept of magic bullet coined by German Nobel Laureate, Paul Ehrlich is the need of the hour when the deadly diseases like cancer has taken over the world [1]. The challenge is to create “smart bomb” which can destroy the tumor cells and prevent the risk of collateral damage [2]. Hydrazone derivatives are used in such treatments where the drug is coupled to antibodies using acid-labile hydrazone bonds [3]. Literature studies reveal that Schiff bases have a wide range of biological properties. Among these some of the fluoro-based Schiff base have been found out to be cytotoxic

concerning the human embryonic cell line (HEL) [4]. Several Schiff base metal complexes are used for second order non-linear optics (NLO). These effects can only be induced by molecules and materials which lacks a centre of symmetry (in order to allow a restoring force which is asymmetric), usually with dipolar D- π -A structure where π is a conjugated system (bridged) [5].

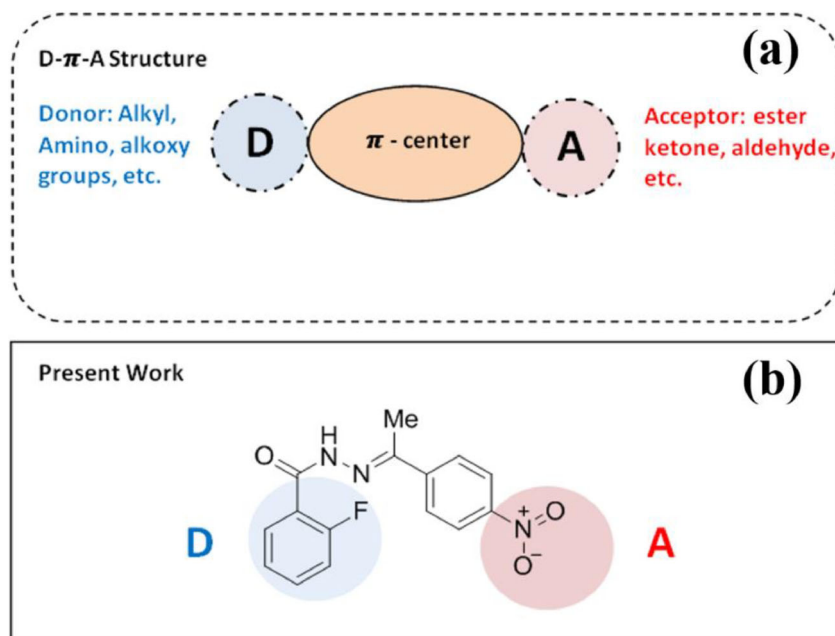
When a molecule absorbs a photon, the electrons of HOMO (Highest Occupied Molecular Orbital) get promoted to LUMO (Lowest Unoccupied Molecular Orbital) which is followed by an intramolecular charge transfer. The excited molecule has a greater dipole moment because of highly polar state which can be accounted from the conformational change that happens upon excitation in comparison to the ground state [6, 7]. The fluorophores are very helpful in order to analyze the microenvironment properties that surround the molecule as they undergo Donor-Acceptor (D-A) molecular bond rotations and the D-A nucleus is responsible for significant charge redistribution upon photoexcitation (Fig. 1a) [7–10]. In order to study this fundamental physical-chemical process in bulk

✉ Anitha Varghese
anitha.varghese@christuniversity.in

¹ Department of Chemistry, Christ (Deemed to be University), Hosur Road, Bengaluru, Karnataka 560029, India

² Department of Chemistry, St Berchmans College (Autonomous), Changanassery, Kerala 686101, India

Fig. 1 (a) The interaction between Donor and Acceptor (D-A) groups and (b) the presence of D-A groups in the chemical structure of FNEB



solution, the determination of ground state dipole moment and excited state dipole moment is of utmost importance as it further helps in the determination of nucleophilic and electrophilic attack sites in some of the photochemical reactions [11]. The knowledge of the excited state dipole moment is useful in determining how a photochemical transformation progresses or to elucidate the nature of the excited state [12]. There are quite a few methods which are available for the determination of electric dipole in different electronic states of a solute molecule in any solvent [13–15]. The most prominent existing method is the one based on change in intensities and the band obtained in the electronic spectra for solvents having different polarities which is called as Solvatochromic method [16, 17].

Solvatochromism can be described using innumerable methods such as the characteristics of the solvent and its spectral parameters [18]. Theories described are based on the specific electrostatic solute-solvent interactions explained by Onsager, where solvent is described as a dielectric continuum hosting the solvent molecules into a cavity which is of Onsager type (Onsager's reaction-field theory) [19]. The theory explains that the solute's electric dipole moment polarizes the solvent so that an electric field is induced; hence the reaction field experienced by the solute is directly proportional to electronic state dipole moment of the compound [20].

In the current study, we report the synthesis of FNEB which is a novel fluoro-based Schiff base containing an electron donor and acceptor group (Fig. 1b). The azomethine ($-C=N-$) derivative is obtained by the condensation of an active carbonyl containing compound with a primary amine. The excitation and emission spectra of FNEB were recorded in fifteen solvents in order of increasing polarities. The dipole moments of ground state and excited state were computed

using the theoretical relations in Solvatochromic approaches. Catalan and Kamlet-Abboud-Taft parameters were determined from multiple linear regression analysis (MLR) in order to study the interaction between the solute and solvent. The dipole moments were also calculated computationally using TD-DFT method.

Experimental and Computational Studies

Materials and Methods

All the chemicals used in the present research work were obtained from Sigma-Aldrich-Merck Limited. FNEB was purified by recrystallization using ethyl alcohol. Thin layer chromatography (TLC) was performed to confirm purity of the synthesized compounds using silica gel coated aluminium plates (Merck). Solvatochromic shift studies were done using spectroscopic graded solvents like methanol, ethanol, butanol, isopropanol, acetonitrile, dimethyl sulphoxide, N, N-dimethylformamide, acetone, dichloromethane, tetrahydrofuran, ethyl acetate, diethyl ether, 1,4-dioxane, n-Hexane and toluene purchased from S-D Fine Chemicals Limited, India. ^1H and ^{13}C NMR were recorded on 400 MHz Bruker NMR using DMSO-d_6 (Dimethyl sulphoxide- d_6) as the solvent and Me_4Si (tetramethylsilane) as the internal standard. Infra Red (IR) spectrum was recorded using Bruker-Alpha-T ATR/FTIR spectrometer. The emission and excitation spectrum were recorded for low concentration (10^{-5} M) of analyte using Shimadzu (UV/Visible 1800) and Shimadzu Spectrofluorometer (RF5301PC). The solvatochromic results were analyzed using OriginPro Software. The relative

permittivity (dielectric constant) of solvent and compound dissolved in the solvent were recorded using Cromtech LCR Meter (Model JC2812B) and refractive indices of compound dissolved in suitable solvent, air and solvent were recorded using Abbe's Refractometer. CHI608 Electrochemical analyzer was used to determine HOMO and LUMO energies experimentally. Theoretical computational study were done using Gaussian 09 W software program where TD-DFT mode was used. TD-DFT computational analyses were used to study the property of surface (nucleophilic or electrophilic sites) in FNEB. These studies were done using Gaussian 09 W software which was also used to optimize the geometry of FNEB in both the electronic states (Fig. 2). The theoretical Light Harvesting efficiency (LHE) was computed using B3LYP/6-31++G(d) basic set. The chemical stability of FNEB was determined using computational and cyclic voltammetry by the use of obtained energy gap between the frontier orbitals.

Theory

The estimation of dipole moments of the electronically singlet excited state (μ_{ex}) and ground state (μ_{gr}) for any organic compound can be determined using both experimentally and theoretically. Guggenheim method is used for determination of experimental ground state dipole moment (μ_{gr}). DFT was also used for determination of the dipole moments in both the states.

Experimental Calculation for Ground State Dipole Moment

The determination of μ_{gr} using E. A Guggenheim method is shown in Eq. (1)

$$\mu_{\text{gr}} = \sqrt{\left[\frac{27KT}{4\pi N(\epsilon_1 + 2)(n_1^2 + 2)} \times \frac{\Delta}{C} \right]} \quad (1)$$

Where C is concentration of solute in a given solvent, $\Delta = (\epsilon_{12} - n_{12}^2) - (\epsilon_1 - n_1^2)$, here ϵ_{12} and n_{12} are relative

permittivity and refractive index of the solution containing solute, ϵ_1 and n_1 are relative permittivity and refractive index of the pure solvent.

Theoretical Calculations for Ground State Dipole Moment

Bilot and Kawski [21, 22] derived expressions for effect of Solvatochromism as a function of both relative permittivity and solvent's refractive index which is shown as

$$\bar{\nu}_{\text{Abs}} - \bar{\nu}_{\text{Flu}} = m^{(1)} f(n, \epsilon) + \text{constant} \quad (2)$$

$$\bar{\nu}_{\text{Abs}} + \bar{\nu}_{\text{Flu}} = -m^{(2)} \varphi(n, \epsilon) + \text{constant} \quad (3)$$

Where $\bar{\nu}_{\text{Abs}}$ and $\bar{\nu}_{\text{Flu}}$ are wave number (cm^{-1}) for absorption and fluorescence respectively and $\varphi(n, \epsilon)$ is given as the sum of solvent polarity functions, i.e., $f(n, \epsilon) + 2g(n)$.

The functions $f(n, \epsilon)$ and $g(n)$ are given using the following expressions

$$f(n, \epsilon) = \frac{\epsilon - 1}{\epsilon + 2} - \frac{n^2 - 1}{n^2 + 2} \frac{2n^2 + 1}{n^2 + 2} \quad (4)$$

$$g(n) = \frac{3}{2} \frac{[n^4 - 1]}{[n^2 + 2]^2} \quad (5)$$

The variables $m^{(1)}$, $m^{(2)}$ are slopes of linear graphs for both Eqs. (2) and (3) of Bilot-Kawski and their values can be given as follows

$$m(1) = \frac{2(\mu_{\text{ex}} - \mu_{\text{gr}})^2}{hca^3} \quad (6)$$

$$m(2) = \frac{2(\mu_{\text{ex}}^2 - \mu_{\text{gr}}^2)}{hca^3} \quad (7)$$

where μ_{gr} and μ_{ex} are the electronic ground and excited state dipole moments of the molecule, "h" is the Planck's constant, 'c' is the velocity of light and 'a' is the Onsager radius. The Onsager cavity can be calculated using Edward's atomic increment method by the use of van der Waal's volume [23].

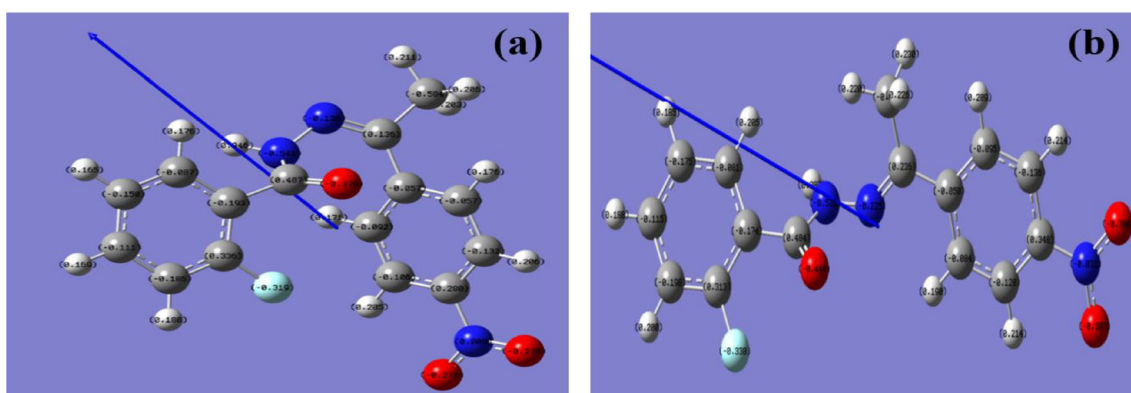


Fig. 2 Optimized geometry of FNEB using TD-DFT in (a) Ground state and (b) Excited state

The Onsager radius is calculated using Eq. (8).

$$a = \sqrt[3]{\left[\frac{3M}{4\pi\delta N_A}\right]} \quad (8)$$

Where the density of the solute is denoted by δ , M is molecular weight and N_A is the Avagadro's number.

Considering that the symmetry of the molecule remains unchanged in both ground and excited states, the dipole moment for both the states are considered as parallel [22]. Based on Eqs. (6) and (7), the following expressions were derived.

$$\mu_{gr} = \frac{m^{(2)} - m^{(1)}}{2} \left[\frac{(hca^3)}{|2m^{(1)}|} \right]^{1/2} \quad (9)$$

$$\mu_{ex} = \frac{m^{(2)} + m^{(1)}}{2} \left[\frac{(hca^3)}{|2m^{(1)}|} \right]^{1/2} \quad (10)$$

$$\mu_{ex} = \mu_{gr} \left[\frac{m^{(1)} + m^{(2)}}{m^{(2)} - m^{(1)}} \right] \quad (11)$$

If the dipole moments μ_{gr} and μ_{ex} are not parallel, then the angle (φ) made is determined using Eq. (12)

$$\cos \varphi = \frac{1}{2\mu_{ex}\mu_{gr}} \left\{ (\mu_{ex}^2 + \mu_{gr}^2) - \frac{m^{(1)}}{m^{(2)}} (\mu_{ex}^2 - \mu_{gr}^2) \right\} \quad (12)$$

Therefore,

$$\varphi = \cos^{-1} \left[\frac{1}{2\mu_{ex}\mu_{gr}} \left\{ (\mu_{ex}^2 + \mu_{gr}^2) - \frac{m^{(1)}}{m^{(2)}} (\mu_{ex}^2 - \mu_{gr}^2) \right\} \right]$$

Experimental Calculations for Dipole Moment in the Excited State

The experimental excited state dipole moment is determined by three separate equations which were suggested by Lippert-Mataga {Eq. (13)} [24, 25], Baksheiv {Eq. (14)} [26] and Kawski-Chamma-Viallet {Eq. (15)} [27, 28] are given below.

$$\bar{\nu}_{Abs} - \bar{\nu}_{Flu} = m_1 P_1 + \text{constant} \quad (13)$$

$$\bar{\nu}_{Abs} + \bar{\nu}_{Flu} = m_2 P_2 + \text{constant} \quad (14)$$

$$\frac{(\bar{\nu}_{Abs} + \bar{\nu}_{Flu})}{2} = m_3 P_3 + \text{constant} \quad (15)$$

Where P_1 , P_2 , P_3 represents the solvent polarity functions {Eqs. (16), (17) and (18)}, m_1 , m_2 and m_3 represent the slopes of the linear relationship {Eqs. (19), (20) and (21)} which can be given as

$$P_1 = \left\langle \frac{\epsilon - 1}{2\epsilon + 1} - \frac{n^2 - 1}{2n^2 + 1} \right\rangle \quad (16)$$

$$P_2 = f(n, \epsilon) \quad (17)$$

$$P_3 = \left[\left(\frac{P_2}{2} \right) + \left(\frac{3(n^4 - 1)}{2(n^2 + 2)^2} \right) \right] \quad (18)$$

The refractive index of the solvent is denoted by 'n' and the relative permittivity by ' ϵ '. The linear plots were plotted using Eqs. (13), (14) and (15) and corresponding slopes m_1 , m_2 and m_3 were obtained which is obtained by the following equations.

$$m_1 = \frac{2(\mu_{ex} - \mu_{gr})^2}{hca^3} \quad (19)$$

$$m_2 = \frac{2(\mu_{ex} - \mu_{gr})^2}{hca^3} \quad (20)$$

$$m_3 = \frac{2(\mu_{ex}^2 - \mu_{gr}^2)}{hca^3} \quad (21)$$

Based on microscopic polarity parameter E_T^N , Reichardt proposed a much improved technique when compared to the regularly used bulk solvent polarity functions [29], which was used to determine μ_{ex} using Eq. (22) and for determining dipole moment change ($\delta\mu$) from ground to excited state.

$$\bar{\nu}_{Abs} - \bar{\nu}_{Flu} = m_4 E_T^N + \text{constant} \quad (22)$$

$$m_4 = 11307.6 \left[\left(\frac{\delta\mu}{\delta\mu_B} \right)^2 \left(\frac{a_B}{a} \right)^3 \right] \quad (23)$$

Where $\delta\mu_B$ is the change in dipole moment of betaine dye and ' a_B ', ' a ' are Onsager radius of betaine and solute molecule respectively. By the use of Eq. (23), the dipole moment for the molecule in the excited state is calculated from Eq. (24)

$$\mu_{ex} = \sqrt{\left[\frac{m_4 81}{11307.6 \left(\frac{6.2}{a} \right)^3} \right]} + \mu_{gr} \quad (24)$$

The electrostatic solute-solvent interactions which are non-specific in nature as described by Onsager is explained using multiple linear regression (MLR) analysis based on linear solvation energy relationship (LSER) [30]. This concept of MLR was proposed by Katritzky and Kamlet-Abboud-Taft [31], which was used for correlation of excitation, emission wavelength, Stoke's shift with hydrogen bond acceptor (β) ability, hydrogen bond donor (α) and the solvents dipolarity/polarizability (π^*) [32] and can be expressed as

$$z = z_0 + a\alpha + b\beta + c\pi^* \quad (25)$$

$$z = z_0 + a \left(\frac{\varepsilon - 1}{2\varepsilon + 1} \right) + b \left(\frac{n^2 - 1}{2n^2 + 1} \right) + cE_T \quad (26)$$

Where z is the Stoke's shift ($\bar{\nu}_{\text{Abs}} - \bar{\nu}_{\text{Flu}}$) and z_0 indicates the physiochemical properties of the shift which does not depend on solvent (in gaseous phase) [$(\bar{\nu}_{\text{Abs}} - \bar{\nu}_{\text{Flu}})_0$]. ε is the dielectric constant/ relative permittivity, n is refractive index and E_T (30) scale is the microscopic solvent polarity parameter for a given solvent. The polarizability of two different interrelated solvents in the solvatochromic shift approach is distinguished by using Catalan method.

Generalized Treatment of Solvent Effect Using Catalan Method

Catalan method was used in MLR to estimate the non-specific solvent effects by splitting the traditional single-parameter into polarizability (SP) term and dipolarity term (SdP) along with solvent acidity (SA) and solvent basicity (SB) [33]. The expression for particular approach is given as below

$$z = z_0 + aSA + bSB + cSP + dSdP \quad (27)$$

Amongst the four coefficients a , b , c and d , d is not prone to any change in its equivalent parameter for the spectroscopic parameter.

Determination of the Quantum Yield (Φ)

Quantum yield of a molecule can be determined using single point method. The integrated fluorescence intensity (I) and optical density (OD) of the compound is compared to optical density (OD_R) and intensity (I_R) of reference (anthracene in ethyl alcohol) at room temperature. Φ is given as Eq. (28)

$$\Phi = \Phi_R \frac{I}{I_R} \frac{OD_R}{OD} \frac{n^2}{n_R^2} \quad (28)$$

Where, Φ_R is quantum yield of reference (standard value of 0.27). The constants n and n_R are the refractive indices of solvent and reference respectively and ratio of squares of n and n_R is assumed to be 1.

Determination of Frontier orbital's (HOMO and LUMO) Energies

Computational Studies The difference in the energies of frontier orbitals, i.e., highest occupied molecular orbital (HOMO) and lowest unoccupied molecular orbital (LUMO) gives the band gap ($E_{\text{HOMO}} - E_{\text{LUMO}}$) for the considered molecule was found out by TD-DFT studies using Gaussian 09 software. TD-DFT/PCM (B3LYP/6-31G (d,p)) mode was used. The geometry of molecule in both ground state and excited state were optimized. Mulliken charges for each atoms were also

generated. Finally, molecular electrostatic potential plot was done to evaluate the electrophilic and nucleophilic sites.

Cyclic Voltammetry Method Typical cyclic voltammograms for the given compound and the internal standard ferrocene were obtained in an organic solvent using lithium perchlorate in acetonitrile as the supporting electrolyte. The electrode system consisted of aqueous silver/silver chloride electrode as reference electrode, Platinum (Pt) electrode as working electrode and platinum counter electrode at ambient temperature is used. HOMO-LUMO was determined using oxidation potential (E_{ox}) values. The energies for HOMO and LUMO were calculated using Eqs. (29) and (30)

$$E_{\text{HOMO}} = -[(E_{\text{ox}} - E_{\text{ferrocene}}) + 4.8] \text{ eV} \quad (29)$$

$$E_{\text{LUMO}} = -[(E_{\text{red}} - E_{\text{ferrocene}}) + 4.8] \text{ eV} \quad (30)$$

$$E_G = -[(E_{\text{HOMO}} - E_{\text{LUMO}})] \text{ eV} \quad (31)$$

Where, E_{HOMO} and E_{LUMO} represent the energies of HOMO and LUMO respectively. $E_{\text{ferrocene}}$ is reduction potential for internal standard ferrocene. E_{red} is reduction potential of the molecule in consideration. The standard value for reduction potential for ferrocene-ferrocenium ion is 4.8 and the electrochemical gap between frontier orbitals energies is given by E_G as shown in Eq. (31).

Global Reactivity Parameters

DFT measures are used in the calculations of global reactivity parameters such as electronegativity (χ), hardness (η) and softness (σ) [34]. Chemical potential (ρ) is known as first order derivative of the electron systems total electronic energy (E) with respect to total electrons (N) at an external potential due to nuclei $V(r)$ [35] or can be defined as the negative value of electronegativity as described by Iczkowski and Margrave [36] as shown in Eq. (32).

$$-\rho = \chi = -\left(\frac{\partial E}{\partial N}\right) V(r) \quad (32)$$

Hardness (η) is defined as the second order derivative of E with N at $V(r)$ that gives an idea about the molecules reactivity and stability by Eq. (33) [37].

$$\eta = -\left(\frac{\partial^2 E}{\partial N^2}\right) V(r) = -\left(\frac{\partial E}{\partial N}\right) V(r) \quad (33)$$

The chemical hardness is calculated by a finite difference approximation to Eq. (33) which is given in Eq. (34). Chemical hardness and electronegativity of the molecule is

also given by Koopmans' theorem [37] and is calculated by the Eqs. (34) and (35).

$$\eta = \frac{IP-EA}{2} = -[E_{LUMO}-E_{HOMO}] \quad (34)$$

$$\chi = \frac{EA + IP}{2} = -[E_{LUMO} + E_{HOMO}] \quad (35)$$

Where IP is the ionization potential (eV) and EA is the electron affinity (eV).

Another global chemical reactivity parameter electrophilicity (ω) was introduced by Parr et al. [38] which is described as Eq. (36) [39].

$$\omega = \frac{\rho^2}{2\eta} \quad (36)$$

Electrophilicity index was defined as a measure of electrophilic power for a considered molecule. The global softness is a reciprocal of hardness [40] as given in Eq. (37).

$$\sigma = \frac{1}{\eta} \quad (37)$$

Total energy change of the molecule is defined as $\Delta E_T = -\eta/4$.

All the above global reactivity parameters were computed by the use of TD-DFT/PCM method.

A molecule or the atoms are said to be electron acceptor, when they possess positive electron affinity and this cause them to undergo charge transfer reactions and the vice versa, i.e., electron donating power measures the IP (energy required for removing an electron from HOMO) of the donor molecule. The difference between EA and IP accounts for the overall energy balance (DE) which accounts for the energy gained/lost in an electron donor/acceptor transfer. The energy balance can be given by the difference of EA and IP. Electronegativity is a chemical property that defines the ability of an atom or a functional group to attract the electron density towards itself. The concept of η tells that a larger E_G accounts for a molecule to be hard and smaller E_G for it to be a soft molecule. This accounts for the fact that the molecule with least E_G is more reactive.

Scheme 1 Synthetic scheme of FNEB



Molecular Electrostatic Potential (MESP)

MESP is used in studying the relation between the structure and activity by the means of electrostatic property [41].

MESP surface diagram can be used to understand the molecules reactive sites wherein the negative regions represent electrophilic sites and the positive regions represent nucleophilic centers.

The identification of key features necessary for the “recognition” of one molecule by another is done by the use of MESP. It is a useful tool in studying both electrophilic and nucleophilic processes [42–45]. At the point r , MESP $V(r)$ is given by Eq. (38).

$$V(r) = Z_A/|R_A-r| \quad (38)$$

Where, $V(r)$ is the electron density at r , Z_A is the charge on the nucleus located at R_A . The first term is due to the nuclear charge and the second is accounted to the electronic distribution.

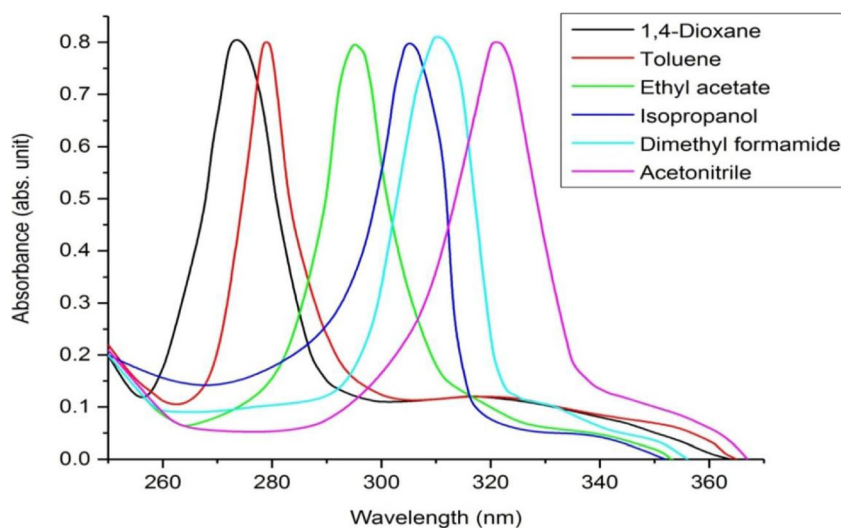
Synthesis of (*E*)-2-Fluoro-N'-(1-(4-Nitophenyl)Ethylidene)Benzohydrazide (FNEB)

An equal amount of 2-fluorobenzohydrazide (1 mmol, 0.154 g), 4-nitroacetophenone (1 mmol, 0.165 g) was taken in a round bottomed flask and 2–3 drops of glacial acetic acid was taken along with ethanol as the solvent. The solution was refluxed for 5 h at 60–70 °C as shown in Scheme 1. The completion of reaction was observed using TLC (with 70% ethyl acetate and 30% n-hexane as solvent system). The crude yellow solid product thus obtained was purified using filtration, washing with cold ethyl alcohol and finally recrystallized using ethyl alcohol.

Characterization of (*E*)-2-Fluoro-N'-(1-(4-Nitophenyl)Ethylidene)Benzohydrazide (FNEB)

Pale yellow crystalline solid; Yield: 79%; mp: 219–220 °C; IR (KBr, cm^{-1}): 3081.16 (Ar C – H str), 1664.66 (C=O str), 1613.45 (C=N str), 1346.73 (C-N str), 1110.24 (N-N str), 1526.68 and 1346.73 (Ar-NO₂); ¹HNMR (d₆-DMSO), δ , ppm): 8.30–7.40 (m, 8H, Ar-H), 7.20 (s, 1H, N-H), 2.50 (s, 3H, CH₃); ¹³CNMR (d₆-DMSO), δ , ppm): 162.2, 160, 151, 144, 127.6, 123.5, 112, 17.

Fig. 3 Excitation spectrum of FNEB in different organic solvents



Results and Discussion

Effects of Solvents on Excitation and Emission Spectra of FNEB

The excitation absorbance (Fig. 3) and emission fluorescence (Fig. 4) spectra were recorded in fifteen solvents ranging from non-polar to polar aprotic and then finally to polar protic solvents at room temperature. The concentration of FNEB was maintained at 10^{-5} M to record its electronic spectra. The $\bar{\nu}_{\text{Abs}}$, $\bar{\nu}_{\text{Abs}} - \bar{\nu}_{\text{Flu}}$ in cm^{-1} , the difference of the two respective wave numbers gave the Stokes shift ($\Delta\nu$) and their sum ($\Sigma\nu$) along with the average of their sum ($\Sigma\nu/2$) for the synthesized compound FNEB were tabulated in Table 1. The polarity functions [$P_1(\epsilon, n)$, $P_2(\epsilon, n)$ and $P_3(\epsilon, n)$] along with

Reichardt's parameter (E_T^N) for the fifteen solvents are given in Table 2.

It is clear from Table 1 that on increase of the solvent polarity, a bathochromic shift takes place with maximum absorption wavelength ranging from 3 nm to 51.5 nm relative to n-hexane due to $\pi-\pi^*$ transition which occurs because of charge transfer of conjugated entity of FNEB. Bathochromic shift ranging from 8 nm to 165 nm relative to n-hexane were observed in maximum fluorescence wavelength, which is attributed to high influence of solvent polarity in the excited state of FNEB compared to its ground state. The Stoke's shift was observed to increase from $12,037.04 \text{ cm}^{-1}$ to $13,434.56 \text{ cm}^{-1}$ with increased solvent polarity from n-hexane and toluene respectively. The above data conclude that FNEB is influenced by solvent polarity

Fig. 4 Emission spectrum of FNEB in different organic solvents

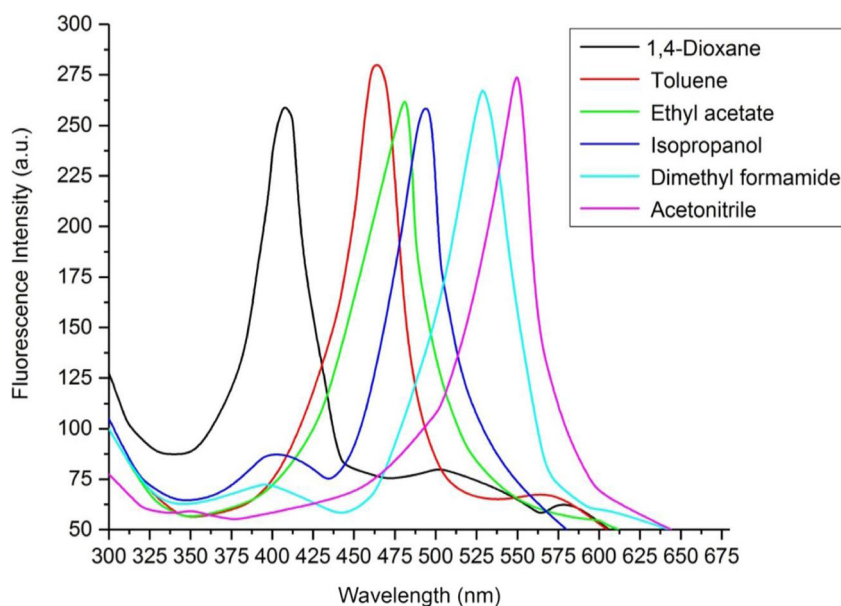


Table 1 Solvatochromic studies of FNEB in different solvents

| Solvents ^a | λ_{Abs} (nm) | ν_{Abs} (cm ⁻¹) | λ_{Flu} (nm) | ν_{Flu} (cm ⁻¹) | $\Delta\nu$ (cm ⁻¹) ($\nu_{\text{Abs}}-\nu_{\text{Flu}}$) | $\Sigma\nu$ (cm ⁻¹) ($\nu_{\text{Abs}} + \nu_{\text{Flu}}$) | $(\Sigma\nu)/2$ (cm ⁻¹) |
|-----------------------|-----------------------------|--|-----------------------------|--|---|---|-------------------------------------|
| Hexane | 270 | 37037.04 | 400 | 25000 | 12037.04 | 62037.04 | 31018.52 |
| 1,4Dioxane | 273 | 36630.03 | 408 | 24509.80 | 12120.23 | 61139.84 | 30569.92 |
| Toluene | 282 | 35460.99 | 454 | 22026.43 | 13434.56 | 57487.42 | 28743.71 |
| Diethylether | 295.5 | 33840.95 | 472 | 21186.44 | 12654.51 | 55027.38 | 27513.69 |
| Ethylacetate | 296 | 33783.78 | 473.5 | 21119.32 | 12664.46 | 54903.11 | 27451.55 |
| Tetrahydrofuran | 300 | 33333.33 | 481.7 | 20757.65 | 12575.68 | 54090.99 | 27045.49 |
| Dichloromethane | 300.5 | 33277.87 | 485.5 | 20597.32 | 12680.55 | 53875.19 | 26937.59 |
| Butanol | 301 | 33222.59 | 490 | 20408.16 | 12814.43 | 53630.75 | 26815.38 |
| Isopropanol | 304 | 32894.73 | 496 | 20161.29 | 12733.45 | 53056.03 | 26528.01 |
| Acetone | 306 | 32679.74 | 504.5 | 19821.61 | 12858.13 | 52501.34 | 26250.67 |
| Ethanol | 310 | 32258.06 | 517 | 19342.36 | 12915.70 | 51600.42 | 25800.21 |
| Methanol | 310 | 32258.06 | 520 | 19230.77 | 13027.30 | 51488.83 | 25744.42 |
| Dimethylformamide | 312 | 32051.28 | 528 | 18939.39 | 13111.88 | 50990.67 | 25495.34 |
| Acetonitrile | 321 | 31152.65 | 549.5 | 18198.36 | 12954.28 | 49351.01 | 24675.51 |
| Dimethyl sulfoxide | 321.5 | 31104.20 | 565 | 18198.36 | 12905.84 | 49302.56 | 24651.28 |

^a Solvents in ascending order of relative permittivity

functions [$P_1(\epsilon, n)$, $P_2(\epsilon, n)$, $P_3(\epsilon, n)$, Reichardt's parameter (E_T^N)], hydrogen bond acceptor (β) ability, hydrogen bond donor (α) and the solvents dipolarity/polarizability (π^*). The excited state of FNEB is stabilized more in polar solvents leading to a higher value of excited state dipole moment compared to that of the ground state dipole moment. Thus, the absorption spectra are least susceptible to the solvent polarity as compared to the emission spectra of FNEB. This was proposed after observing weak bathochromic shift in the absorption spectra.

Experimental and Theoretical Calculations of Dipole Moments for FNEB

The experimental dipole moment for the ground state was determined by Guggenheim Debye method using Eq. (1) and was found out to be 2.58 D. Density functional Theory (DFT) based on B3LYP/6-31G(d) were used to estimate ab-initio dipole moments of both ground state and the excited state which was found out to be $\mu_{\text{gr}} = 2.10$ D and $\mu_{\text{ex}} = 7.33$ D. The spectral parameters were correlated in the solvatochromic studies of FNEB with the use of different

Table 2 Solvent polarity functions along with the Reichardt's parameter for solvents

| Solvent | Lippert-Mataga $P_1(\epsilon, n)$ | Bakhsheiv $P_2(\epsilon, n)$ | Kawski-Chamma-Viallet $P_3(\epsilon, n)$ | Reichardt Parameter E_T^{N4} |
|--------------------|-----------------------------------|------------------------------|--|--------------------------------|
| n-Hexane | 0.0013 | 0.0024 | 0.2550 | 0.009 |
| 1,4-Dioxane | 0.0204 | 0.0414 | 0.3074 | 0.164 |
| Toluene | 0.0132 | 0.0290 | 0.3499 | 0.099 |
| Diethylether | 0.1647 | 0.3707 | 0.4253 | 0.117 |
| Ethylacetate | 0.1993 | 0.4879 | 0.4973 | 0.228 |
| Tetrahydrofuran | 0.2088 | 0.5466 | 0.5499 | 0.207 |
| Dichloromethane | 0.2171 | 0.5903 | 0.5829 | 0.321 |
| Butanol | 0.2641 | 0.7532 | 0.6479 | 0.602 |
| Isopropanol | 0.2700 | 0.7624 | 0.6434 | 0.546 |
| Acetone | 0.2848 | 0.7925 | 0.6404 | 0.355 |
| Ethanol | 0.2888 | 0.8131 | 0.6525 | 0.654 |
| Methanol | 0.3085 | 0.8544 | 0.6509 | 0.762 |
| Dimethylformamide | 0.2752 | 0.8393 | 0.7116 | 0.839 |
| Acetonitrile | 0.2632 | 0.8409 | 0.7444 | 0.841 |
| Dimethyl sulfoxide | 0.3057 | 0.8615 | 0.6637 | 0.862 |

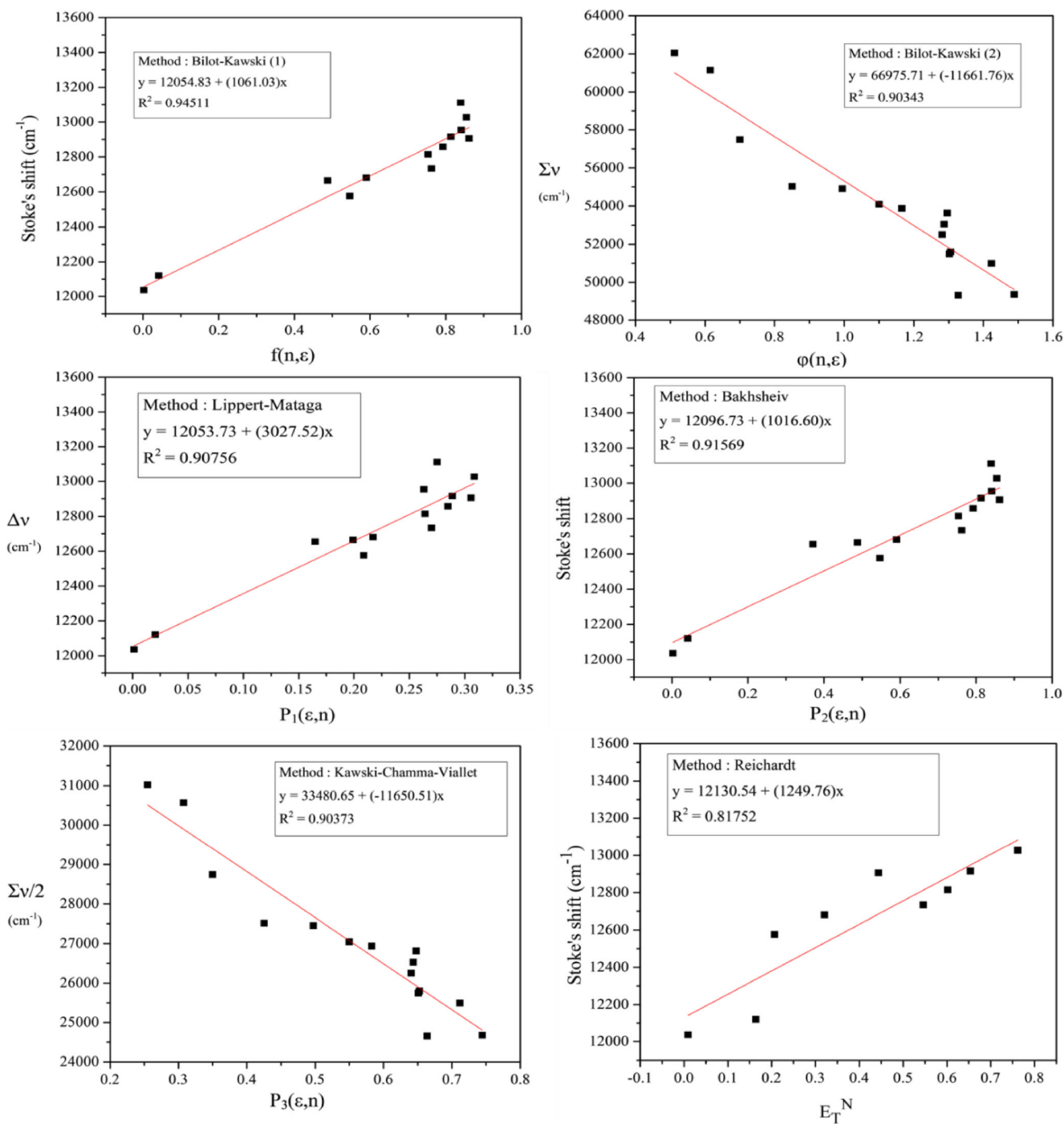


Fig. 5 Linear plots of solvent polarity functions $f(\epsilon, n)$, $\varphi(\epsilon, n)$, $P_1(\epsilon, n)$, $P_2(\epsilon, n)$, $P_3(\epsilon, n)$ and E_T^N against $(\bar{\nu}_{Abs} - \bar{\nu}_{Flu})$, $(\bar{\nu}_{Abs} + \bar{\nu}_{Flu})/2$

solvent polarity approaches. The linear graphs for Bilot-Kawski, Lippert-Mataga, Bakhshiev, Kawski-Chamma-Viallet and Reichardt methods were plotted as shown in Fig. 5, where $(\bar{\nu}_{Abs} - \bar{\nu}_{Flu})$ and $(\bar{\nu}_{Abs} + \bar{\nu}_{Flu})/2$ were plotted against $f(\epsilon, n)$ and $\varphi(\epsilon, n)$ respectively, Stoke's shift, its mean $\{(\bar{\nu}_{Abs} - \bar{\nu}_{Flu})\}$ and $\{(\bar{\nu}_{Abs} + \bar{\nu}_{Flu})/2\}$ for FNEB (Table 1) were plotted against solvent polarity functions (Table 2).

Table 3 summarizes the obtained linear equation from all the correlation approaches and from the slopes and intercepts

obtained from Fig. 5, the dipole moments of FNEB in both ground and excited states were calculated. The Correlation coefficient values which are high (generally greater than 0.90) suggests a good linear relationship for the above correlation methods. The dipole moment in ground state and excited state were calculated using quantum-mechanical treatment of Bilot-Kawski using Eqs. (9) and (10). Incorporating Eq. (19) to (21) and (24), the other correlation methods were used to calculate excited state from respective slopes m_1 , m_2 , m_3 ,

Table 3 Linear plots for various correlation methods for FNEB

| Method | General linear equation $y = mx + C$ | Slope m | Intercept C | Correlation Coefficient R^2 | N^a |
|-----------------------------|--|------------|---------------|-------------------------------|-------|
| Bilot-Kawski ⁽¹⁾ | $\bar{\nu}_{\text{Abs}} - \bar{\nu}_{\text{Flu}} = m^{(1)} f(n, \epsilon) + C \{2\}$ | 1061.03 | 12054.83 | 0.94511 | 13 |
| Bilot-Kawski ⁽²⁾ | $\bar{\nu}_{\text{Abs}} + \bar{\nu}_{\text{Flu}} = -m^{(2)} \varphi(n, \epsilon) + C \{3\}$ | -116661.76 | 66975.71 | 0.90343 | 15 |
| Lippert-Mataga | $\bar{\nu}_{\text{Abs}} - \bar{\nu}_{\text{Flu}} = m_1 P_1 + C \{13\}$ | 3027.52 | 12053.73 | 0.90756 | 14 |
| Bakhshiev | $\bar{\nu}_{\text{Abs}} - \bar{\nu}_{\text{Flu}} = m_2 P_2 + C \{14\}$ | 1016.6 | 12096.73 | 0.91569 | 14 |
| Kawski-Chamma-Viallet | $\frac{(\bar{\nu}_{\text{Abs}} + \bar{\nu}_{\text{Flu}})}{2} = m_3 P_3 + C \{15\} \frac{(\text{Abs} + \text{Flu})}{2}$ | -11650.51 | 33480.65 | 0.90373 | 15 |
| Reichardt | $\bar{\nu}_{\text{Abs}} - \bar{\nu}_{\text{Flu}} = m_4 E_T^N + C \{22\}$ | 1249.76 | 12130.54 | 0.81752 | 9 |

^a Number of data

m_4 , as given in Table 4. Onsager cavity radius (a) was determined using Eq. (8). By the use of Eq. (28), quantum yield (φ) of FNEB was found out to be 0.23.

From Table 4, it was found out that μ_{ex} of FNEB is greater than μ_{gr} . The calculated values for the excited state dipole moment (μ_{ex}) using Bilot-Kawski⁽²⁾, Baksheiv and Reichardt approaches are unanimous. The higher values for other approaches in the determination of μ_{ex} can be attributed for the polarizability effect due to the solute. The phenomenon of charge transfer (CT) can account for the difference in dipole moments and nature of the excited state. Using Eqs. (9) and (10), ground state dipole moment (μ_{gr}) and excited state dipole moment (μ_{ex}) of FNEB were calculated (Bilot-Kawski approach) considering both the dipole moments to be parallel [16]. The value of μ_{gr} obtained from Gaussian software as well as Bilot-Kawski⁽¹⁾ are unanimous. The dipole moments for both the states as given by Bilot-Kawski are $\mu_{\text{gr}} = 1.30$ D and $\mu_{\text{ex}} = 1.56$ D suggesting that the excited state of FNEB has charge separation and thus becomes more polar to the ground state which can be attributed to stronger solute-solvent interaction in case of electronically excited state. Using Eq. (11), $\mu_{\text{ex}}/\mu_{\text{gr}}$ (ratio of dipole moments) was found to be 0.83.

Multiple Linear Regression (MLR) Analysis

The solute-solvent interaction and the electronic transition mechanism are studied using multiple linear regression analysis (MLR). It is known that these interactions interfere with the shape, intensity and position of the absorption spectra. The influences of solvents in the

absorption and fluorescence spectra were determined by the use of both Kamlet-Abboud-Taft and Catalan parameters. These parameters were correlated to determine solvatochromic properties of FNEB.

Kamlet-Taft parameters α , β and π^* are determined using Eq. (25). Catalan parameters include polarizability (SP) term and dipolarity term (SdP) along with solvent acidity (SA) and solvent basicity (SB) as shown in Eq. (27). The values of these parameters are given in Table 5.

The values of $\bar{\nu}_{\text{Abs}}$, $\bar{\nu}_{\text{Flu}}$, $\Delta\nu$ were correlated with the parameters using MLR. The electronic transition mechanisms between both the electronic states were analyzed, which is on the basis of solute-solvent interactions.

The regression analysis with correlation coefficient for FNEB using Kamlet-Abboud-Taft parameters is given in Eq. (39).

$$\left. \begin{aligned} \bar{\nu}_A &= 36766.76 - 466.47\alpha - 1802.85\beta - 4240.38\pi^*; R^2 = 0.96 \\ \bar{\nu}_F &= 24649.98 - 674.91\alpha - 2059.02\beta - 4900.73\pi^*; R^2 = 0.95 \\ \Delta\bar{\nu} &= 12116.69 + 208.61\alpha - 255.51\beta + 660.96\pi^*; R^2 = 0.88 \end{aligned} \right\} \quad (39)$$

The regression analysis with correlation coefficients for FNEB using Catalan parameters is given in Eq. (40).

$$\left. \begin{aligned} \bar{\nu}_A &= 35814.25 + 281.78\text{SA} - 313.00\text{SB} + 2072.28\text{SP} - 5584.12\text{SdP}; R^2 = 0.90 \\ \bar{\nu}_F &= 24359 - 295.16\text{SA} + 9.64\text{SB} + 609.47\text{SP} - 6174.23\text{SdP}; R^2 = 0.87 \\ \Delta\bar{\nu} &= 12681.91 + 101.39\text{SA} - 117.62\text{SB} - 1026.84\text{SP} + 930.15\text{SdP}; R^2 = 0.82 \end{aligned} \right\} \quad (40)$$

From Eq. (39), it can be observed that a slightly higher π^* coefficient is obtained than the other coefficients of α and β .

Table 4 Dipole moments (μ_{gr} and μ_{ex}) for FNEB

| a (\AA) | Method for calculating Dipole moments (in Debye) | | | | | | | | |
|----------------------|--|-------------------|-------------------|-----------------------------|-----------------------------|-------------------|-------------------|-----------------------|-------------------|
| | Guggenheim | Gaussian | | Bilot-Kawski ⁽¹⁾ | Bilot-Kawski ⁽²⁾ | Lippert Mataga | Bakhshiev | Kawski-Chamma-Viallet | Reichardt |
| | μ_{gr} | μ_{gr} | μ_{ex} | μ_{gr} | μ_{ex} | μ_{ex} | μ_{ex} | μ_{ex} | μ_{ex} |
| 4.15 | 2.58 | 2.10 | 7.33 | 1.30 | 1.56 | 8.29 | 2.94 | 9.47 | 6.94 |

Table 5 Kamlet-Abboud-Taft and Catalan parameters values for MLR analysis

| MLR | Kamlet-Abboud-Taft | | | Catalan parameters | | | |
|--------------|--------------------|---------|---------|--------------------|-------|-------|-------|
| | α | β | π^* | SA | SB | SP | SdP |
| Hexane | 0 | 0 | -0.081 | 0 | 0.056 | 0.616 | 0 |
| 1,4Dioxane | 0 | 0.37 | 0.55 | 0 | 0.444 | 0.737 | 0.312 |
| Toluene | 0 | 0.11 | 0.54 | 0 | 0.128 | 0.782 | 0.284 |
| Diethylether | 0 | 0.47 | 0.27 | 0 | 0.562 | 0.617 | 0.385 |
| Ethylacetate | 0 | 0.45 | 0.55 | 0 | 0.542 | 0.656 | 0.603 |
| THF | 0 | 0.55 | 0.58 | 0 | 0.591 | 0.714 | 0.634 |
| DCM | 0.3 | 0 | 0.82 | 0.04 | 0.17 | 0.76 | 0.769 |
| Butanol | 0.79 | 0.88 | 0.47 | 0.341 | 0.809 | 0.674 | 0.655 |
| Isopropanol | 0.76 | 0.84 | 0.48 | 0.283 | 0.83 | 0.633 | 0.808 |
| Acetone | 0.08 | 0.48 | 0.71 | 0 | 0.475 | 0.651 | 0.907 |
| Ethanol | 0.83 | 0.77 | 0.54 | 0.4 | 0.658 | 0.633 | 0.783 |
| Methanol | 0.93 | 0.62 | 0.6 | 0.605 | 0.545 | 0.608 | 0.904 |
| DMF | 0 | 0.69 | 0.88 | 0.031 | 0.613 | 0.759 | 0.977 |
| Acetonitrile | 0.19 | 0.31 | 0.75 | 0.044 | 0.286 | 0.645 | 0.974 |
| DMSO | 0 | 0.76 | 1 | 0.072 | 0.647 | 0.83 | 1 |

Therefore, using MLR analysis, it can be observed that the solvent dipolarity/polarizability (π^*) has a vital influence on the interactions between the solute and the solvent. This implies that π^* controls the excitation as well as the emission spectra as π^* is more powerful than β and α . On the other hand, the relatively higher values of β cannot be neglected as the value is greater than α . The fairly higher values for π^* and β indicate that both the absorption and fluorescence spectra show bathochromic shift. The comparatively greater π^* and β in the emission spectral wavenumber $\bar{\nu}_{\text{Flu}}$ than the excitation spectral wavenumber $\bar{\nu}_{\text{Abs}}$ of FNEB indicates

a more polarized state in excited state than the ground state. This leads to a higher μ_{ex} value. MLR using Catalan parameter, dipolarity term (SdP) from Eq. (40) indicates a red shift. In comparison to the excitation dipolarizability, the emission dipolarizability influences the interactions between the solute and solvent suggesting a higher value of dipole moment of FNEB in its excited state. Using MLR analysis, it can be shown that $\bar{\nu}_{\text{Abs}}$ and $\bar{\nu}_{\text{Flu}}$ have relatively good correlation coefficients. The above results conclude solvents play a major role in the intramolecular charge transfer which is due to the polarizability/dipolarizability parameter of a particular solvent.

Determination of Frontier orbital's Energies

The frontier orbitals namely Highest Occupied Molecular Orbital (HOMO) and Lowest Unoccupied Molecular Orbital (LUMO) will give insights into the direction of charge transfer (CT). The energies of frontier orbitals were determined in ethanol. The energies give necessary details concerning CT and explains electron donor/acceptor ability where HOMO is responsible for the electron donor ability whereas LUMO for the electron acceptor ability. The difference in the energies (HOMO-LUMO energy gap) of both gives detail about the properties of the molecule's chemical stability.

Determination of Frontier orbital's Energies Using Computational Method

The red and green colored lobes correspond to positive phase and negative phase. It was observed that HOMOs for both ground state and excited state of FNEB are localized on azomethine linkage and carbonyl group of

Fig. 6 (a) The ground state HOMO (b) ground state LUMO (c) excited state HOMO and (d) excited state LUMO, for FNEB were computed by TD-DFT studies

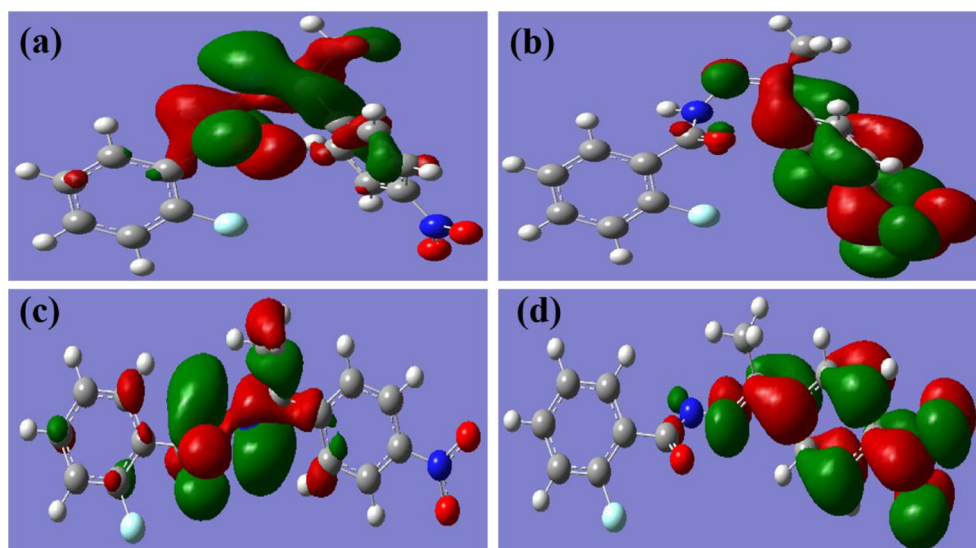


Table 6 Global reactivity parameters of FNEB

| Method | | Hardness η (eV) | Softness (eV) | Electronegativity Index χ (eV) | Chemical Potential μ (eV) | Electrophilicity Index ω (eV) |
|--------|------------------|----------------------|---------------|-------------------------------------|-------------------------------|--------------------------------------|
| TD-DFT | (g) ^a | 1.92 | 0.52 | 1.92 | -4.95 | 6.38 |
| | (e) ^b | 0.88 | 1.13 | 0.88 | -4.81 | 13.14 |
| CV | | 0.20 | 5.11 | 0.20 | 4.77 | 58.20 |

^a TD-DFT method for the ground state of FNEB, ^b TD-DFT method for the excited state of FNEB

ortho-fluorobenzoyl moiety whereas LUMOs for both the states of FNEB are localized over the entire molecule except for 2-fluorobenzene nucleus (Fig. 6). Using the values of HOMO and LUMO energies for both ground and excited states, the global reactivity parameters were found out using Eqs. (32), (34), (35), (36) and (37) and have been tabulated in Table 6.

The suitable position for the electrophilic and nucleophilic attack can be determined from the MESP plot (Fig. 7).

MESP can also be used to study the influence of solvents by means of hydrogen bonding. The scale for MESP symbolizes different potentials on the surface of FNEB molecule, which is electrostatic in nature. The red color represents negative phase (electrophilic site) whereas blue color represents positive phase (nucleophilic site). The carbonyl group and nitro group are susceptible to electrophilic attack as they are in the red/negative phase. The blue/positive phases are enclosed by the methyl group, benzene ring containing fluoro, imine group and all the hydrogens.

Determination of Frontier Orbital Energies Using Cyclic Voltammetry

HOMO and LUMO energies were also determined using cyclic voltammetry using the Eqs. (29) and (30) and the energy gap (E_G) was calculated. The cyclic voltammograms of FNEB and the internal standard ferrocene were recorded in acetonitrile where lithium perchlorate was used as the supporting electrolyte and shown in Fig. 8. HOMO-LUMO energies were determined using the reduction and oxidation potential values.

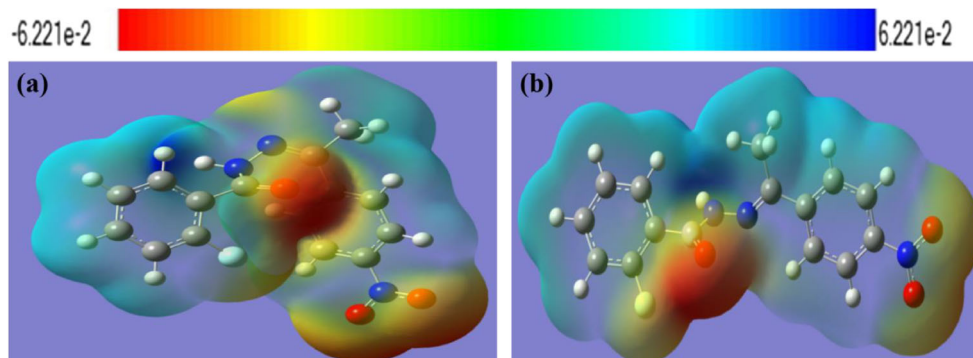
HOMO (E_{HOMO}) and LUMO (E_{LUMO}) energies determined in acetonitrile were found to be 0.18 and 0.17 a.u. respectively. Global reactivity parameters were calculated using the HOMO and LUMO energies from the redox potential values determined using cyclic voltammetry (CV) and given in Table 6.

The use of Gaussian 09 gave insights into the charge distribution in FNEB from atomic charges of each atom in the optimized geometry (Fig. 2). The study was done in ethyl alcohol. In case of ground state, O atoms (8, 13, 14), all nitrogen apart from (N-7) and C (2,3,4,5,6,15,18,19,20,21) atoms have a significant negative charge and act as donor atoms. The C atoms (1, 9, 12, 17) and N (7) atoms carry significant positive charge, thereby acting as acceptor atoms. The charge distribution direction in solvent medium directs from C (12) to N (11) atom having magnitude +0.487 to -0.540 eV respectively in case of ground state whereas the direction of the charge distribution in case of the excited state is from C (9) to N (11) atom having magnitude +0.236 to -0.541 eV respectively. FNEB is more polar giving rise to difference in dipole moments of both the states as there is charge separation. The positive charge in all the hydrogen atoms indicate electron donating character of hydrogen compared to rest of the atoms. The above studies confirm the conclusions obtained from MLR analysis.

Light Harvesting Studies

Light Harvesting Efficiency (LHE) of a molecule is a very important physical property, which indicates the

Fig. 7 Molecular electrostatic potential (MESP) plot for FNEB (a) Ground state and (b) Excited state



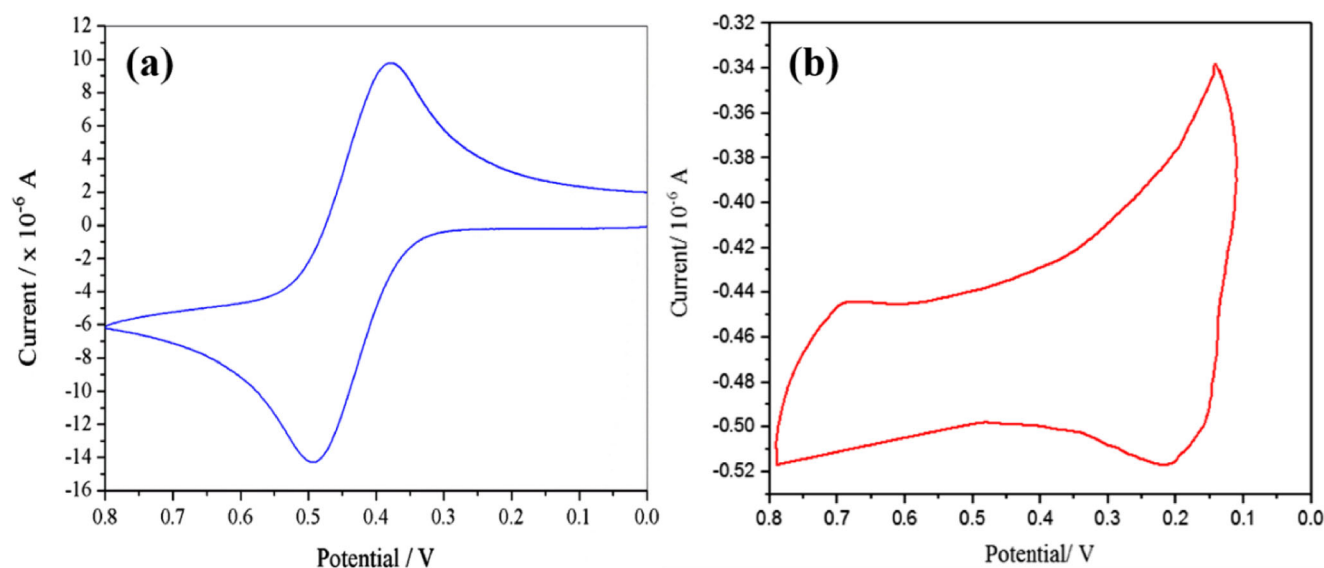


Fig. 8 Cyclic voltammograms of (a) Internal standard ferrocene and (b) FNEB

use of compounds in conventional Dye Sensitized Solar Cells (DSSC's) for converting light energy to electrical energy. The LHE is mathematically related to the oscillating strength through the equation $LHE = 1 - 10^{-A}$, where A is the oscillating strength corresponding to the UV excitation valuates obtained from the TD-DFT calculations. The results of TD-DFT calculations using B3LYP/6-31++G(d) in ethanol as solvent using i.e. fPCM model is provided in Table 7. There are three major transitions corresponding to wavelength 707.54 and 425.43 nm with oscillator strength 0.2195 and 0.1851 respectively. The calculated LHE is 0.52 and 0.34, which suggests that the in the first transition, 52.08% of energy is can be transferred to the conducting material in DSSC by photosensitization, while in second, only 34.70% of light energy can only be transferred.

Conclusion

The influence in excitation and emission spectra by solvents of different polarities are computed using solvent polarity correlation methods. The optimized geometries of FNEB in ground and excited states were achieved using TD-DFT. The dipole moments in excited state

was found to be higher than that in ground state based on quantum-mechanical treatment of Bilot-Kawski approach. Density functional Theory (DFT) based ab-initio estimation of dipole moments also indicated the same. All the correlation methods indicated that the excited state of FNEB has charge separation and thus more polar when compared to the ground state accounting for stronger solute-solvent interaction in case of electronically excited state. Multiple Linear Regression analysis using both Kamlet-Abboud-Taft and Catalan parameters suggested that the polarity term (π^*) of solvents is responsible in controlling the excitation and emission spectra. The frontier orbitals energies were calculated computationally using TD-DFT calculations and cyclic voltammetry. The Light harvesting efficiency which was determined to gain insights into the photovoltaic property of the molecule confirms the energy transfer of about 52.08% to conducting material in DSSC by photosensitization in the first transition whereas it decreased in the second transition.

The energies of the frontier orbitals were used to calculate the global reactivity parameters which give information about the surface of FNEB. MESP plots explain that the molecule has nucleophilic/electrophilic sites. Based on the results obtained, FNEB can be considered as a potentially suitable candidate for designing

Table 7 Light Harvesting studies of FNEB

| No. | Energy (cm-1) | Wavelength (nm) | Oscillation Strength | LHE | Symmetry | Major contributions |
|-----|---------------|-----------------|----------------------|----------|-----------|---------------------|
| 1 | 14133.35 | 707.5463 | 0.3195 | 0.520819 | Singlet-A | HOMO- > L + 1 (92%) |
| 2 | 23505.58 | 425.4309 | 0.1851 | 0.34702 | Singlet-A | HOMO- > L + 2 (86%) |

materials for luminescence and fluorescent probe applications.

Acknowledgements The authors would like to thank Anthem Biosciences for FTIR and NMR analyses. The authors express heartfelt gratitude to Indian Institute of Science (IISc), Bengaluru, India for performing the computational analysis.

Funding This research did not receive any specific grant from funding agencies in the public, commercial, or not-for-profit sectors.

References

- Drews J (2004) Paul Ehrlich: Magister Mundi. *Nat Rev Drug Discov* 3:797–801. <https://doi.org/10.1038/nrd1498>
- Strebhardt K, Ullrich A (2008) Paul Ehrlich's magic bullet concept: 100 years of progress. *Nat Rev Cancer* 8:473–480. <https://doi.org/10.1038/nrc2394>
- Laguzza BC, Nichols CL, Briggs SL, Cullinan GJ, Johnson DA, Starling JJ, Baker AL, Bumol TF, Corvalan JRF (1989) New anti-tumor monoclonal antibody-vinca conjugates LY203725 and related compounds: design, preparation, and representative in vivo activity. *J Med Chem* 32:548–555. <https://doi.org/10.1021/jm00123a007>
- Jarrahpour A, Khalili D, Clercq ED, Salmi C, Brunel JM (2007) Synthesis, antibacterial, antifungal and antiviral activity evaluation of some new bis-Schiff bases of Isatin and their derivatives. *Molecules* 12:1720–1730. <https://doi.org/10.3390/12081720>
- Rigamonti L (2010) Schiff base metal complexes for second order nonlinear optics. *La Chim I'Industria Soc Chim Ital* 3:118–122
- Grabowski ZR, Rotkiewicz K, Rettig W (2003) Structural changes accompanying intramolecular Electron transfer: focus on twisted intramolecular charge-transfer states and structures. *Chem Rev* 103:3899–4032. <https://doi.org/10.1021/cr9407451>
- Hayashi R, Tazuke S, Frank CW (1987) Pressure effects on the twisted intramolecular charge transfer (TICT) phenomenon. *Chem Phys Lett* 135:123–127. [https://doi.org/10.1016/0009-2614\(87\)87228-7](https://doi.org/10.1016/0009-2614(87)87228-7)
- Paczkowski J, Neckers DC (1991) Twisted intramolecular charge-transfer phenomenon as a quantitative probe of polymerization kinetics. *Macromolecules* 24:3013–3016. <https://doi.org/10.1021/ma00010a059>
- Bajorek A, Paczkowski J (1998) Influence of the attachment of chromophores to a polymer chain on their twisted intramolecular charge-transfer state in dilute solution. *Macromolecules* 31:86–95. <https://doi.org/10.1021/ma970378q>
- Alphonse R, Varghese A, George L, Nizam A (2016) Estimation of ground state and excited state dipole moments of a novel Schiff base derivative containing 1, 2, 4-triazole nucleus by solvatochromic method. *J Mol Liq* 215:387–395. <https://doi.org/10.1016/j.molliq.2015.12.050>
- Kumari R, Varghese A, George L, KB A (2016) Photophysical study of 6-amino-3-methyl-4-(4-nitrophenyl)-1,4-dihydropyran[2,3-c]pyrazole-5-carbonitrile and estimation of ground-state and singlet excited-state dipole moments by solvatochromic approaches. *J Mol Liq* 222:828–835. <https://doi.org/10.1016/j.molliq.2016.07.133>
- Zakerhamidi MS, Ahmadi-Kandjani S, Moghadam M, Ortyl E, Kucharski S (2012) Solvatochromism effects on the dipole moments and photo-physical behavior of some azo sulfonamide dyes. *Spectrochim Acta Part A Mol Biomol Spectrosc* 85:105–110. <https://doi.org/10.1016/j.saa.2011.09.042>
- Czekalla J (1960) Elektrische Fluoreszenz-polarisation: Die Bestimmung von Dipolmomenten angeregter Moleküle aus dem Polarisationsgrad der Fluoreszenz in starken elektrischen Feldern. *Berichte Der Bunsengesellschaft Für Phys Chemie* 64:1221–1228. <https://doi.org/10.1002/bbpc.19600641016>
- Kawski A, Kukliński B, Bojarski P (2005) Dipole moment of aniline in the excited S1 state from thermochromic effect on electronic spectra. *Chem Phys Lett* 415:251–255. <https://doi.org/10.1016/j.cplett.2005.09.008>
- Czekalla J (1961) Zwei Elektro-Optische Methoden Zur Bestimmung Von Dipolmomenten Angeregter Moleküle. *Chimia* 15:26–31
- Patil SK, Wari MN, Panicker CY, Inamdar SR (2013) Solvatochromic study of coumarin 545 in alcohols for the determination of ground and excited state dipole moments. *Int J Adv Res* 1:616–626
- Rauf MA, Hisaindee S (2013) Studies on solvatochromic behavior of dyes using spectral techniques. *J Mol Struct* 1042:45–56. <https://doi.org/10.1016/j.molstruc.2013.03.050>
- Nicol MF (1974) Solvent effects on electronic spectra. *Appl Spectrosc Rev* 8:183–227. <https://doi.org/10.1080/05704927408060375>
- Joshi S, Pant DD (2012) Ground and excited state dipole moments of quinine sulfate dication: Solvatochromic shift of absorption and fluorescence spectra. *J Mol Liq* 172:125–129. <https://doi.org/10.1016/j.molliq.2012.04.002>
- Sharma R, Joshi S, Bhattacharjee R, Pant DD (2015) Solvent effect on absorption and fluorescence spectra of cinchonine and cinchonidine dications: estimation of ground and excited state dipole moments by experimental and numerical studies. *J Mol Liq* 206:159–164. <https://doi.org/10.1016/j.molliq.2015.02.002>
- Bilot L, Kawski A (1962) Zur Theorie des Einflusses von Lösungsmitteln auf die Elektronenspektren der Moleküle. *Zeitschrift Für Naturforsch A* 17:621–627. <https://doi.org/10.1515/zna-1962-0713>
- Kawski A, Rabek JF (1992) Progress in photochemistry and photophysics, 5th edn. CRC Press, Boca Raton
- Akshaya KB, Varghese A, Lobo PL, Kumari R, George L (2016) Synthesis and photophysical properties of a novel phthalimide derivative using solvatochromic shift method for the estimation of ground and singlet excited state dipole moments. *J Mol Liq* 224:247–254. <https://doi.org/10.1016/j.molliq.2016.09.115>
- Lippert E, Naturforsch Z (1955) The solvent effect on the spectral shift. *Phys Sci* 10:541–545
- Mataga MKN, Kaifu Y (1945) Berichte der Bunsengesellschaft für physikalische Chemie. *Chem Soc Jpn* 29:465–470
- Bakshiev NG (1964) Universal intermolecular interactions and their effect on the position of the electronic spectra of molecules in two component solutions. *Opt Spektrosk* 16:821–832
- Kawski A (1966) der Wellenzahl von elektronenbanden lumineszierenden moleküle. *Acta Phys Pol* 29:507–518
- Chamma A, Viallet PCR (1970) Determination du moment dipolaire d'une molecule dans un etat excite singulet. *CR Acad Sci Paris Ser C* 270:1901–1904
- Reichardt C (1994) Solvatochromic dyes as solvent polarity indicators. *Chem Rev* 94:2319–2358. <https://doi.org/10.1021/cr00032a005>
- Benchea AC, Babusca D, Morosanu AC, Dimitriu DG, Dorohoi DO (2017) Spectral study of rhodamine dyes in binary solutions. *J Mol Struct* 1140:71–76. <https://doi.org/10.1016/j.molstruc.2016.12.091>
- Fowler FW, Katritzky AR, Rutherford RJD (1971) The correlation of solvent effects on physical and chemical properties. *J Chem Soc B Phys Org* 0:460. <https://doi.org/10.1039/j29710000460>
- Kamlet MJ, Abboud JLM, Abraham MH, Taft RW (1983) Linear solvation energy relationships. 23. A comprehensive collection of

- the solvatochromic parameters, ρ , α , and β , and some methods for simplifying the generalized solvatochromic equation. *J Org Chem* 48:2877–2887. <https://doi.org/10.1021/jo00165a018>
33. Catalán (2009) Toward a generalized treatment of the solvent effect based on four empirical scales: Dipolarity (SdP, a new scale), polarizability (SP), acidity (SA), and basicity (SB) of the medium. *J Phys Chem B* 113:5951–5960. <https://doi.org/10.1021/jp8095727>
34. Fu J, Zang H, Wang Y, Li S, Chen T, Liu X (2012) Experimental and theoretical study on the inhibition performances of Quinoxaline and its derivatives for the corrosion of mild steel in hydrochloric acid. *Ind Eng Chem Res* 51:6377–6386. <https://doi.org/10.1021/ie202832e>
35. Parr RG, Donnelly RA, Levy M, Palke WE (1978) Electronegativity: the density functional viewpoint. *J Chem Phys* 68:3801–3807. <https://doi.org/10.1063/1.436185>
36. Iczkowski RP, Margrave JL (1961) Electronegativity. *J Am Chem Soc* 83:3547–3551. <https://doi.org/10.1021/ja01478a001>
37. Parr RG, Pearson RG (1983) Absolute hardness: companion parameter to absolute electronegativity. *J Am Chem Soc* 105:7512–7516. <https://doi.org/10.1021/ja00364a005>
38. Parr RG, Szentpály LV, Liu S (1999) Electrophilicity index. *J Am Chem Soc* 121:1922–1924. <https://doi.org/10.1021/ja983494x>
39. Chattaraj PK, Roy DR (2007) Update 1 of: Electrophilicity index. *Chem Rev* 107:PR46–PR74. <https://doi.org/10.1021/cr078014b>
40. Lesar A, Milošev I (2009) Density functional study of the corrosion inhibition properties of 1,2,4-triazole and its amino derivatives. *Chem Phys Lett* 483:198–203. <https://doi.org/10.1016/j.cplett.2009.10.082>
41. Sheela NR, Muthu S, Sampathkrishnan S (2014) Molecular orbital studies (hardness, chemical potential and electrophilicity), vibrational investigation and theoretical NBO analysis of 4-(1H-1,2,4-triazol-1-yl)methylene dibenzonitrile based on abinitio and DFT methods. *Spectrochim Acta Part A Mol Biomol Spectrosc* 120:237–251. <https://doi.org/10.1016/j.saa.2013.10.007>
42. Kolandaivel P, Praveena G, Selvarengan P (2005) Study of atomic and condensed atomic indices for reactive sites of molecules. *J Chem Sci* 117:591–598. <https://doi.org/10.1007/bf02708366>
43. Luque FJ, López JM, Orozco M (2000) Perspective on “electrostatic interactions of a solute with a continuum. A direct utilization of ab initio molecular potentials for the prevision of solvent effects”. *M Theor Chem Acta* 103:343–345. <https://doi.org/10.1007/s002149900013>
44. Okulik N, Jubert AH (2005) Theoretical analysis of the reactive sites of non-steroidal anti-inflammatory drugs. *Internet Electron J Mol Des* 4(1):17–30
45. Özdemir N, Eren B, Dinçer M, Bekdemir Y (2010) Experimental and ab initio computational studies on 4-(1H-benzo[d]imidazol-2-yl)-N,N-dimethylaniline. *Mol Phys* 108:13–24. <https://doi.org/10.1080/00268970903476688>

Publisher's Note Springer Nature remains neutral with regard to jurisdictional claims in published maps and institutional affiliations.